

## Preparation and evaluation of biodegradable double-layer insert of Sulfacetamide sodium for ocular drug delivery

Haider H. Kikawoos<sup>1,\*</sup>, Athmar DH. H. Al-Shohani<sup>2</sup>

Received 9<sup>th</sup> Nov. 2024, Accepted 20<sup>th</sup> Feb. 2025, Published: xx<sup>rd</sup> xxx, 202x, DOI: <https://doi.org/10.xxxx>

Accepted Manuscript, In press

**Abstract:** A key challenge in ocular medication administration is attaining a therapeutic drug concentration at the site of action for a prolonged duration. The present study employed the antibacterial Sulfacetamide in a biodegradable ocular insert to achieve prolonged drug release. The inserts were prepared using solvent casting for the matrix and dipping technique for the rate-controlling layer. The polymers utilized were medium-viscosity sodium alginate, polyvinyl pyrrolidone K90, and Eudragit RLPO. All developed inserts were assessed for folding durability, thickness, drug content, swelling capacity, and an in vitro release study. The formulation including 1.5% (w/v) sodium alginate and 7% (w/v) PVP K90 as the matrix, alongside a rate-controlling layer of 15% (w/v) Eudragit RLPO and 5% (w/v) PVP K90, was identified as the optimum formula, demonstrating a prolonged drug release over 12 hours with zero-order release kinetics. Furthermore, a score of zero was noted in the ocular irritation assessment, alongside a four-fold increase in ocular drug absorption via goat cornea. This innovative polymeric composite may decrease the frequency of drug administration from 8-12 times, as observed with standard sulfacetamide eye drops, to merely twice daily while maintaining an adequate therapeutic dose.

**Keywords:** Biodegradable, ocular drug delivery, ocular film, Sulfacetamide.

### Introduction

Bacterial infections constitute a major category of ocular diseases, including conjunctivitis, endophthalmitis, keratitis, blepharitis, dacryocystitis, and orbital cellulitis. Bacterial conjunctivitis, sometimes referred to as "pink eye," is frequently encountered in primary health clinics, where the individuals are presented with ocular redness, and mostly coupled with ocular discomfort, itching, and discharge. Additionally, bacterial conjunctivitis contributes to elevated morbidity and might presented in a more complicated scenarios for clinicians(1).

Sulfacetamide (SAC) is widely used in the management of ocular topical infections owing to its antibacterial properties. This class of sulfonamide antimicrobial agents has bacteriostatic properties and show broad-spectrum activity mostly against Gram-positive and some Gram-negative pathogens. It serves as a competitive antagonist to para-aminobenzoic acid, inhibiting its conversion into folic acid, a key metabolite for bacterial nucleic acid synthesis, consequently hindering bacterial growth(2).

A major difficulty in ocular drug delivery is to attain and sustain the drug concentration at the therapeutic level at the site of action while ensuring prolonged drug release duration(3). Traditionally, extending the contact duration of ophthalmic formulations with the ocular surface can markedly enhance their residence length and, consequently, their therapeutic effectiveness. Various strategies are employed to address this issue, including the use of viscosity-enhancing agents in eye drop formulations or the development of a water-insoluble ointment. Regrettably, these approaches yield only a marginally prolonged drug release relative to traditional eye drop solutions, and a highly viscous formulation may induce ocular irritation and pose challenges in dosing and application(4).

Moreover, these traditional dosage forms require more frequent administrations daily while being continuously eliminated from the ocular surface by tear formation and nasolacrimal drainage, thereby drastically reducing drug bioavailability to 1-7%(5).

The practical challenges described in the preceding paragraph have majorly driven the pursuit of innovative ocular drug delivery systems, such as ocular inserts, which serve as a means for the release of one or more pharmacologically active ingredients. These inserts can be described as sterile, thin, multi-layered, drug-loaded devices with solid or semi-solid consistency, designed for insertion in the cul-de-sac or conjunctival sac(6).

Compared to conventional ophthalmic formulations such as eye drops, ocular inserts generally offer advantages including improved ocular retention, dosing precision, diminished systemic absorption, decreased frequency of administration, targeted delivery to internal ocular tissues via the non-corneal route (conjunctival), regulated drug release, and extended drug shelf life.(7)

Inserts are categorized as insoluble, soluble, or biodegradable according to their solubility, and the medicine released from the insert is dependent upon diffusion, osmosis, and bio-erosion(8).

One example of an ocular insert is Lacrisert® (5 mg of hydroxypropyl cellulose), which is used to treat moderate to severe dry eye conditions. Lacrisert is a sterile cylindrical dosage form manufactured by Merck, Sharp, and Dohme in 1981. It generally dissolves after 24 hours; hence it does not require removal following the designated insertion duration(9).

1 Department of Pharmaceutics, College of Pharmacy, Mustansiriyah University, Baghdad, Iraq.

\*Corresponding author email: haider\_hussain@uomustansiriyah.edu.iq

2 E-mail: athmar1978@uomustansiriyah.edu.iq

Recent research focused on developing ocular inserts for controlled and extended drug release; specifically, a combination of hot-melt extrusion and 3D printing was employed to create ocular inserts containing ciprofloxacin-HCl, which offer a sustained release profile for a minimum of 24 hours, followed by complete degradation after insertion(10).

The current research seeks to effectively produce a SAC insert that facilitates extended drug release along with complete biodegradation after total drug release.

## Materials and Methods

### Materials

Sulfacetamide Sodium (SAC) (TCI chemicals, Japan) (purity: 99%), PVP K90 (purity: 98% M.W: 360 kDa), eudragit (Eu.) RLPO (Shanghai Macklin Biochemical co, China) (purity: 98% M.W: 32 kDa), dibutyl phthalate (DP) (Heowns, China) (purity: 99%), sodium alginate (Alg.) (Sigma-Aldrich, Germany) (purity: 99% Viscosity: 2000 cps), polyethylene glycol 400 (PEG), sodium chloride (NaCl), sodium bicarbonate (NaHCO<sub>3</sub>), calcium chloride (CaCl<sub>2</sub>) (Loba Chemie, India) (purity: 98%) and marketed product (M.P) Locula (Sulfacetamide Sodium 10%) eye drops from local pharmacy. All other chemical reagents and solutions used were of an analytical grade.

### Methods

#### Inserts preparation:

Inserts were formulated according to weight/volume percentages as outlined in Table (1) . The solvent-casting technique was employed to fabricate the desired inserts. Initially, 20 ml of deionized water (D.W) was preheated to 60 °C, and the physical mixture of SAC-matrix polymers was thereafter introduced into the D.W and vigorously stirred at 1400 rpm using a magnetic hot plate stirrer for 30 minutes. The stirring procedure continued, and 30% w/w PEG 400 (plasticizer) was incorporated based on the total polymeric weight of the insert. Following 30 minutes of stirring, the polymeric dispersion was allowed to settle to room temperature and subsequently stored at 2-4°C for 24 hours to facilitate optimal polymer swelling and hydration. Then the stored polymeric dispersion was warmed up at room temperature for 4 hours, after which 18 ml of the dispersion was cast in a cylindrical plastic Petri dish measuring 1 cm in height and 6 cm in diameter. The cast mixture was dried at room temperature for 72 hours. The drying process formed a thin, flexible polymeric film, which was further cut using a round, sharp-edged steel borer to attain the final specified dimension of a 10 mm diameter circular insert(11).

The inserts formed in the preceding steps were immersed for 5 seconds in 10 ml of an ethanolic solution containing the rate-controlling membrane-forming polymers, together with 10% w/w of DP as a plasticizer (Table (1)). Subsequently, they were allowed to dry for one day at room temperature and thereafter stored in a desiccator for further assessment. The final insert consisted of a thin and flexible polymeric film comprising a matrix layer encased by a rate-controlling layer(12).

**Table (1):** Composition of SAC inserts.

F	Matrix layer w/v			Rate control layer w/v	
	SAC	PVP K90	Alg.	Eu. RL PO	PVP K90
1	1	3	1.5	-	-
2	1	7	1.5	-	-
3	1	10	1.5	-	-
4	1	7	1.5	5	-
5	1	7	1.5	10	-
6	1	7	1.5	15	-
7	1	7	1.5	-	5
8	1	7	1.5	-	10
9	1	7	1.5	-	15
10	1	7	1.5	15	5

#### Physical appearance:

The evaluation of the developed ocular inserts was conducted visually, focusing on surface roughness, shape, size, and color.

#### Thickness:

The mean and standard deviation of ten inserts have been calculated to confirm thickness uniformity. The thickness of each insert was measured at three distinct places using a digital vernier caliper (Shanghai, China) (13).

#### Weight variation:

A weight variation test was conducted using an electronic balance (Kern ALS 220-4N-Germany), and the mean weight of five randomly selected inserts from each batch was measured, and the standard deviation was recorded (14).

#### Surface PH:

The prepared inserts were immersed in 1 ml of distilled water for fifteen minutes, after which a pH meter (HANNA, USA) was directly applied to their surface. The resultant values were documented. This procedure was executed for three randomly chosen inserts from each batch; their pH values were averaged, and the standard deviation was calculated(15).

#### Folding endurance:

is an assessment utilized to evaluate the flexibility and foldability of an insert post-insertion. The test was conducted by repeatedly folding the insert between the index and thumb until it exhibited signs of fracture and cracking, with the total number of folds recorded as the folding endurance value(16).

#### Drug content:

For each produced batch, ten randomly selected inserts were utilized for the SAC content analysis. Each insert was immersed in 100 ml of tear-simulated fluid (TSF) consisting of 0.67 g NaCl, 0.2 g NaHCO<sub>3</sub>, 0.008 g CaCl<sub>2</sub>, and distilled water to a total volume of 100 ml at 37°C for 24 hours with continuous stirring. A solution sample was filtered using a 0.45 µm Whitman filter and analyzed at 257 nm with a UV-VIS spectrophotometer, from which the average drug content for each batch was determined(17).

### Swelling index percent (SI%):

A vacant steel threaded mesh was weighed and subsequently immersed in TSF. An ocular insert was weighed in its dry state and placed on the mesh, with the combined weight of the dry insert and the mesh recorded as the initial weight. The loaded mesh was extracted from the TSF at specified intervals and reweighed after carefully eliminating any surface moisture; this weight was designated as the final weight. The swelling index percentage (SI %) was computed using the formula provided below(18):

$$S.I \% = \frac{\text{Final weight} - \text{Initial weight}}{\text{Initial weight}} \times 100$$

### In vitro release study:

A study was conducted using a Franz diffusion cell with a 22 ml receptor compartment and a 5 ml donor compartment, separated by a dialysis membrane with a molecular weight cut-off of 12,000-14,000 Da, to evaluate the release of the produced inserts and a marketed product (M.P.). The dialysis membrane was immersed in TSF for 24 hours prior to application(19). The insert was positioned in the receptor compartment with 100  $\mu$ l of TSF, while the receptor compartment was filled with TSF and maintained at a temperature of 37°C  $\pm$  0.5°C. One milliliter of solution was extracted from a sampling opening in the receptor compartment and simultaneously substituted with one milliliter of TSF, with this procedure being repeated frequently every hour for a duration of 12 hours (20). The drawn sample was analyzed for drug content using a UV-VIS spectrophotometer at 257 nm following filtration using a 0.24-micrometer syringe filter(21).

### Drug Release Kinetics:

The kinetics of drug release were analyzed for the formulated inserts. The mathematical kinetic models utilized in the research were zero-order kinetics, first-order kinetics, Korsmeyer-Peppas, and Higuchi. This task is carried out by DDSolver. The kinetic model exhibiting the highest coefficient of correlation was chosen(22).

### Ex vivo Bio adhesion:

This test involved fixing goat conjunctival tissue to a stationary plastic platform using cyanoacrylate adhesive, while the ocular insert was secured to a separate, freely movable platform. The conjunctival tissues were surgically removed using a clip from goat eyeballs obtained from a local slaughterhouse. The film-holding platform was firmly placed on the tissue-holding platform with gentle, constant finger pressure for one minute. The mobile platform was attached to a delicate yet firm plastic filament and suspended from an iron stand. At the opposite end of the plastic filament, a plastic container with a specified weight was connected. Upon completion of the preceding procedure, water was introduced into the plastic container via a glass burette at a rate of two drops per second. The test endpoint was achieved when the film was detached from the tissue, and the collected water was weighed and designated as bioadhesive strength, while the force of adhesion and bond strength were calculated using the following formulas(23):

$$\text{Force of adhesion (N)} = (\text{Bioadhesive strength (g.)} \times 9.81 \text{ gravity acceleration})/1000$$

$$\text{Bond strength (N m}^{-2}\text{)} = \text{Force of adhesion/film surface area}$$

### Ex vivo drug permeation study:

the same methodology employed in the in vitro release study was utilized, substituting goat corneal tissue for the dialysis membrane. A surgical clip was utilized to remove this tissue and several segments of the scleral tissues from goat eyeballs freshly obtained from a local slaughter. The acquired tissue was thoroughly rinsed with a cold 0.9% (w/v) normal saline solution to be sure the tissue surface was devoid of proteins. the tissue was positioned so that the corneal surface oriented towards the donor compartment of the Franz cell (24). A graph illustrating cumulative drug release against time was generated from the ex vivo permeation data, and several parameters were computed as follows(25):

1. Steady-state drug flux (Jss)  $\frac{\mu\text{g}}{\text{cm}^2 \cdot \text{h}}$  as the slope of the fitted linear curve.
2. Lag time (Tlag) Determined by extrapolating the fitted linear curve to the x-axis.

### Mechanical characteristics:

The evaluations were performed utilizing the ASTM International Test Method for Thin Plastic Sheeting (D 882-02) texture analyzer (Tinius Olsen UK). A film specimen of 40 x 20 mm was secured by two steel grips; the initial distances between the grips were recorded, along with the separation speed of the grips. The test endpoint was attained when the film ruptured, and the maximum distance between the grips at that instant was recorded. Tensile strength (TS) and percent elongation at the breakage point (E%) were computed using the following formulas(26):

$$\text{Tensile Strength} = \frac{\text{force of break (N)}}{\text{Cross sectional area (mm}^2\text{)}}$$

$$E\% = \frac{D_f - D_0}{D_0} \times 100$$

Where D0 is the initial distance between the grips and Df is the distance between the grips at the breakage point.

### Sterility test and post-UV evaluations:

All inserts were prepared under aseptic settings using pre-sterilized instruments and then exposed to UV radiation for one hour in a UV hood(27). An evaluation of the sterilized inserts was undertaken to confirm that no alterations in physical or chemical characteristics occurred. Trypticase Soy Agar (TSA) and Thioglycollate Broth (TB) were utilized to verify the sterility of the insert. A sterile swab was collected from both insert sides and the edges for inoculation onto TSA, while the inserts were directly submerged in the liquid medium of TB. Both mediums were incubated at 30–35°C and monitored for 14 days for any microbial growth(28).

### Ocular irritation test:

The ocular irritation test was conducted in accordance with the Draize test and as outlined in the OECD Test Guideline 405 (Test No. 405: Acute Eye Irritation/Corrosion 2017), and the Institutional Ethical Committee of Department of Pharmacy, Mustansiriyah University reviewed and approved the protocol (no.31). The test was performed to verify that the insert was non-irritating to ocular tissues due to its distinct polymeric composition, extended exposure to the insert, and the eye's sensitive nature(29). Six healthy White New Zealand rabbits,

each weighing between 1.8 and 2.0 kg, were properly chosen. An individual insert was positioned in the upper conjunctival sac of the left eye of each animal after delicately retracting the upper eyelid from the eyeball and thereafter applying gentle pressure to secure the insert's stable location. The right eye served as the control for the experiment. The eye with the insert was observed for irritation at 1, 6, 12, 18, 24, 48, and 72 hours following insertion(30). The irritation was evaluated using the grading system established in ISO-10993-10(31). Symptoms of ocular irritation or injury to the cornea, iris, and conjunctivae, such as aberrant discharge, conjunctival hyperemia, edema, and corneal opacity, were noted and evaluated using a 3-point scale (0 = no alteration, 1 = mild alteration, 3 = obvious alteration)(32).

### FTIR and DSC Compatibility Study:

FTIR spectroscopy was performed separately on both the drug and polymers, followed by a comparison with the final optimal formulation using the pressed disc technique. The potassium bromide dispersion technique was employed to ascertain the IR absorption spectra of SAC. This procedure involved combining the tested substance with potassium bromide salt, and the resulting physical mixture was compressed using a manual hydraulic press. A round and compressed pellet is generated from the former procedure, which is then positioned in a sample container within the FTIR device and scanned across the wave number range of 400–4000  $\text{cm}^{-1}$  (33). The primary absorption peaks were documented and compared with previously published data(34).

For the DSC analysis, a sample of approximately 3–6 mg was placed in a sealed, flat-bottomed aluminum pan and heated

at a scanning rate of 10°C/min to a maximum temperature of 300°C under nitrogen purge gas, during which the thermal behavior of each component was recorded individually and subsequently compared to the thermal behavior of the final optimal formula(35).

### Stability studies:

A selection of optimal inserts were stored in a sealed glass jar within a desiccator containing varying concentrations of sodium chloride to maintain relative humidity levels of 60%  $\pm$  5% at a temperature of 25°  $\pm$  2°C for 90 days in order to assess the effects of environmental factors such as humidity and temperature(36). The inserts were assessed for thermal properties initially and at thirty-day intervals. Additionally, mechanical properties, surface pH, folding endurance, drug content, and percentage of drug content were examined (37).

### Statistical analysis:

All data shown represent the mean of three measurements, accompanied by  $\pm$  standard deviations. A one-way analysis of variance (ANOVA) was used for statistical analysis, with  $p < 0.05$ , which implies a significant difference.

## Results and Discussion

### General evaluation

All inserts were assessed for folding endurance, pH, weight variation, thickness, drug content, and percentage of drug content (Table 2).

**Table (2):** SAC inserts evaluation parameters and results of all prepared formulations.

F	Folding endurance	pH	Weight variation(mg)	Thickness(mm)	Drug content(mg)	content percentage (%)
1	Over300	6.97 $\pm$ 0.02	34.26 $\pm$ 1.64	0.22 $\pm$ 0.03	4.79 $\pm$ 0.22	95.81 $\pm$ 4.47
2	Over300	6.94 $\pm$ 0.01	63.41 $\pm$ 1.01	0.44 $\pm$ 0.08	4.67 $\pm$ 0.32	93.43 $\pm$ 6.50
3	124 $\pm$ 14.06	6.99 $\pm$ 0.02	74.76 $\pm$ 0.79	0.46 $\pm$ 0.05	5.07 $\pm$ 0.27	101.30 $\pm$ 5.43
4	Over300	6.96 $\pm$ 0.02	75.18 $\pm$ 1.02	0.46 $\pm$ 0.05	4.78 $\pm$ 0.36	95.52 $\pm$ 7.21
5	Ove 300	6.96 $\pm$ 0.01	78.09 $\pm$ 1.01	0.49 $\pm$ 0.04	4.73 $\pm$ 0.28	94.63 $\pm$ 5.66
6	Over300	6.97 $\pm$ 0.02	81.30 $\pm$ 1.21	0.53 $\pm$ 0.06	4.68 $\pm$ 0.39	93.70 $\pm$ 7.84
7	75 $\pm$ 7.12	6.93 $\pm$ 0.02	71.34 $\pm$ 1.54	0.44 $\pm$ 0.04	4.60 $\pm$ 0.35	91.97 $\pm$ 6.94
8	73 $\pm$ 10.40	6.95 $\pm$ 0.01	81.59 $\pm$ 2.12	0.54 $\pm$ 0.07	4.93 $\pm$ 0.46	98.57 $\pm$ 9.18
9	61 $\pm$ 11.43	6.96 $\pm$ 0.02	93.66 $\pm$ 1.77	0.59 $\pm$ 0.07	5.17 $\pm$ 0.39	103.32 $\pm$ 7.82
10	Over300	6.98 $\pm$ 0.02	84.10 $\pm$ 1.42	0.54 $\pm$ 0.05	4.89 $\pm$ 0.29	97.75 $\pm$ 5.89

The developed films were circular, consistent in appearance, slightly yellowish, and smooth in texture. They exhibited no evidence of surface imperfections, roughness, or phase separation between the matrix and the drug, indicating uniform drug distribution(38).

Their diameter was 10 mm, conforming to the permissible maximum diameter of 10 mm (39).

Their thickness values varied from 0.22 mm to 0.59 mm, falling within the permissible range of 0.3 to 1 mm(40).

The recorded surface pH ranged from 6.93 to 6.99, which is within the acceptable range of 6.5 to 7.5; hence, it can be confidently asserted that no ocular irritation is anticipated(41, 42).

Most of the evaluated inserts demonstrated appropriate folding endurance (exceeding 300), suggesting acceptable mechanical resistance to deformation. So, these prepared

inserts can be effortlessly handled and positioned within the conjunctival sac without compromising the film's integrity(43). Still, F3, F7, F8, and F9 failed to pass the folding endurance test due to their elevated PVP K90 concentration.

The test for SAC content yielded values between 4.60 and 5.17 mg, with a percentage range of 91.97% to 103.32%. These results conform to the accepted pharmacopeial standards for drug content uniformity, which is 85% to 115%, and exhibit a low standard deviation that is within allowed ranges(44, 45).

The results demonstrate consistent weight across the formed films, as evidenced by a low standard deviation, suggesting effective homogenization and uniform distribution of the medication and polymer within the film(46).

All polymers exhibited nontoxicity and biocompatibility, and all developed inserts complied with the specified pH range, thickness, and drug content (41).

### Swelling index percent (SI%):

The water absorption or swelling index percentage following the placement of an ocular insert in TSF indicates the hydrophilic or hydrophobic characteristics of the polymeric composite(45). It is regarded as a determinative factor in drug disintegration and release, linked with the host's acceptance, indicating whether it would elicit a foreign sensation during placement. Moreover, effective water absorption and a certain level of surface degradation can facilitate the creation of a smooth-surfaced insert, enabling optimal integration with adjacent tissue post-insertion and minimizing the risk of rejection or expulsion. Excessive swelling or surface degradation (excessive particle leaching) can undermine the insert's capacity to adhere to surrounding tissues and induce a foreign body sensation(47).

F1-F3 exhibited a SI% over 240% accompanied by significant polymer leaching. The extreme swelling exceeding 100% due to fast polymer leaching may induce an unpleasant foreign body sensation in the eye. Furthermore, F4-F7 exhibited a maximum SI% compared to F1-F3, but with tolerable polymer leaching, resulting in incomplete degradation due to its Eud. RLPO content(48). In the meantime, F7, F8, and F9 attained a maximum SI% of around 94%, yet exhibited an unsatisfactory fast polymer leaching comparable to F1-F3 owing to their elevated PVP K90 concentration. In the end, F10 achieved a satisfactory maximum SI% of 98% within 50 minutes, subsequently declining steeply over time. Overall, the combination of PVP K90 with Eud. RLPO resulted in a rate-controlling layer that produced a firm yet flexible insert, efficiently resisting excessive swelling while enabling appropriate polymer leaching, as illustrated in Figure 1(49).

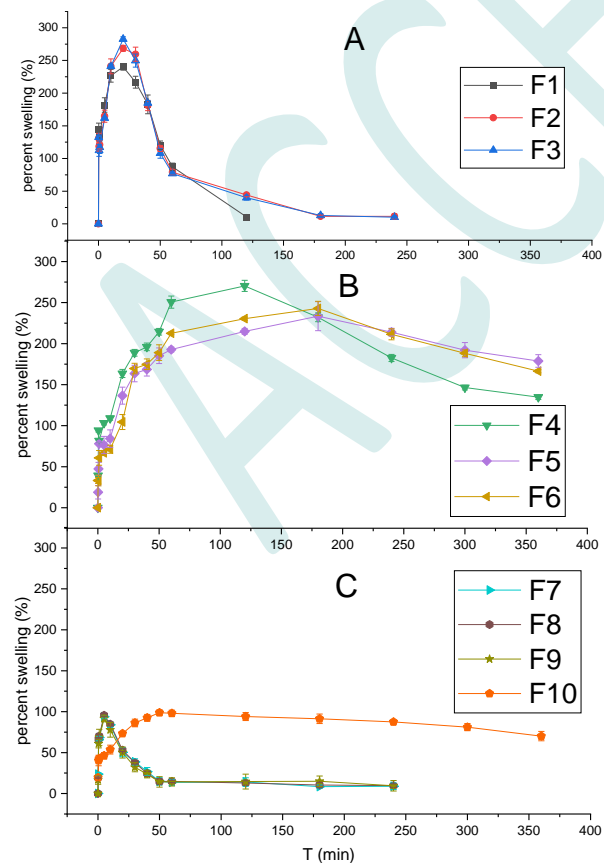


Figure (1): Curved plots of inserts swelling index percent (SI%)

### In vitro release study and Kinetics:

A gradual extension in drug release duration from 3 to 5 hours was seen when comparing F2 to F1, attributable to the incremental rise in PVP K90 concentration from 3% to 7% within the matrix. Based on prior events, a preliminary conclusion was reached to elevate the PVP K90 by up to 10%, similar to F3, with the expectation of prolonging the drug release duration beyond 5 hours (Figure 2-A). Nonetheless, the attempts were regarded as unsuccessful due to the characterization of SAC as a highly water-soluble drug; consequently, it was swiftly solubilized and extricated from the polymeric matrix, particularly in instances involving a polymeric matrix composed exclusively of hydrophilic polymers such as PVP K90 and Alg. The insert design was modified by incorporating a rate control layer composed of Eud RLPO, a hydrophobic polymer, with the intention of facilitating slower water ingress and prolonging duration(50).

Fortunately, F4, F5, and F6 greatly boosted drug release times (6 hours, 8 hours, and 12 hours, respectively) while generally maintaining the desired characteristics and folding endurance. Nevertheless, it did not achieve complete degradation owing to its Eud. RL PO content (Figure 2-B) (48).

The formulation efforts were once again focused on creating a PVP K90-based rate-controlling layer, utilizing the precise percentages of F4, F5, and F6 to achieve complete insert biodegradation and prolonged drug release time. The previously stated modification implemented in F7, F8, and F9 was classified as a failure due to a limited SAC release duration comparable to that observed in F3, leading to the conclusion that PVP K90 cannot function by itself as the rate-controlling layer, even at elevated concentrations (Figure 2-C)(51).

The latest data strongly indicates the necessity of using hydrophobic polymers such as Eud. RL PO, along with a high polymer-to-SAC ratio. Consequently, a potential alteration is proposed for the fabrication of the rate-controlling layer by combining 5% PVP K90 and 15% Eud RLPO to achieve complete biodegradation, as demonstrated in F4, and prolonged drug release in F6 (52). Fortunately, the recent adjustment to produce F10 has granted SAC an extended-release duration of roughly 12 hours, accompanied by complete biodegradation of the insert.

The M.P *in vitro* release analysis indicated a drug release period of only 30 minutes; hence, F6 and F10 were deemed more advantageous formulations for subsequent investigations (Figure 2-D)

based on the recent investigations indicate that both F6 and F10 support the reduction of drug administration frequency from twelve times, as seen in typical eye drop solutions, to a regimen of twice daily(53). Nonetheless, the release profile between F6 and F10 exhibits no significant difference ( $P > 0.05$ ).

The optimal model for F6 and F10 was identified as zero-order release kinetics, exhibiting regression square values of 0.9884 and 0.974, respectively, as presented in Table 3. The drug release mechanism can be understood by the overall polymeric swelling, which facilitated a regulated SAC release, as seen by the swelling behavior of F10, which was marked by a steeply declining plateau following the attainment of its maximum swelling index (54).

Nevertheless, the insert may experience a complex intertwining event, commencing with gradual surface degradation, followed by water infiltration, which induces polymeric swelling and relaxation. Subsequently, the water penetrates the core layer,

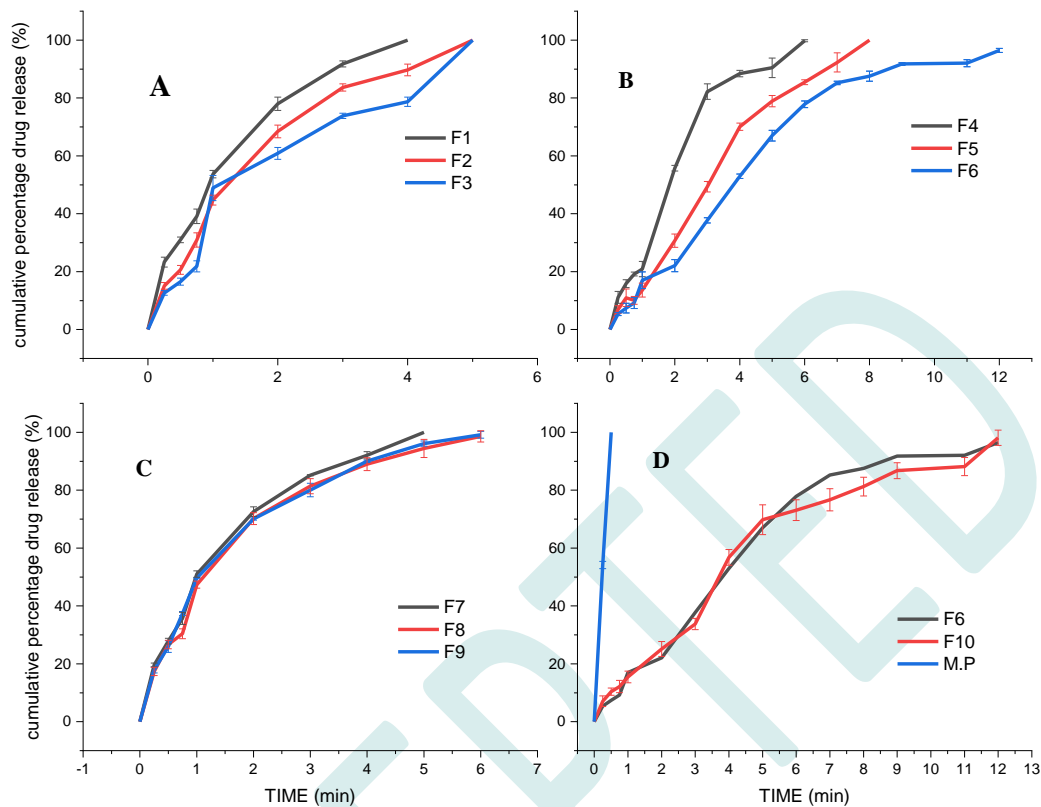


**Figure (2):** Plots of In vitro drug release study A-C) among all the tested formulations. D) optimized F6 and F10 VS. marketed product (M.P)

solubilizing the drug and creating an osmotic gradient. Consequently, the drug release is osmotically regulated and consistently managed through the surface holes created by swelling and degradation(47).

**Table (3):** Release kinetic data of F6 and F10 ocular inserts

Optimum formula		F6	F10
Zero-order	$K_0$	13.118	13.583
	$R_{sqr}$	0.9884	0.974
First-order	$K_1$	0.179	0.188
	$R_{sqr}$	0.9571	0.9385
Higuchi	$K_{H}$	23.341	24.266
	$R_{sqr}$	0.8182	0.8170
Korsmeyer-Peppas	$K_{kp}$	13.262	14.524
	$n$	0.975	0.919
	$R_{sqr}$	0.9795	0.9542

Note: regression square value ( $R_{sqr}$ ), zero-order release constant ( $K_0$ ), first-order release constant ( $K_1$ ), Higuchi diffusion constant ( $K_H$ ), Korsmeyer-Peppas constant ( $K_{kp}$ ), diffusional release exponent ( $n$ )

In summary, this zero-order kinetic drug release behavior provides a consistent drug release devoid of daily fluctuations, hence reducing any adverse effects.

### Ex vivo Bio adhesion:

Ex vivo bio adhesion was conducted for F6 and F10, since both exhibited prolonged drug release of around 12 hours.

Both formulations exhibited an ex vivo bio-adhesive strength of  $0.183 \pm 0.016$  g and  $0.422 \pm 0.014$  g and an adhesion force of  $0.083 \pm 0.016$  N and  $0.187 \pm 0.011$  N, respectively. A significant increase ( $P < 0.05$ ) in both bio-adhesion strength and force of adhesion was reported when comparing F10 with F6, and this enhancement in ex vivo bio-adhesion is likely attributable to its PVP K90 content in the rate-controlling layer and its bio-adhesive characteristics. Furthermore, the bio-adhesive characteristics of the insert can be linked to the cationic charge provided by the EUD. The RLPO of protonated amino  $NH_4^+$  that interacts with the counter anionic charge of the mucus layer that envelops the conjunctiva(55).

According to the acquired data, F10 exhibited an average detachment force above 0.2N, sufficient to offset the force exerted by eyelids during blinking. This value signifies that the produced films will remain localized and attached throughout the insertion period(56).

### Ex vivo drug permeation study

The ex vivo drug permeation study revealed that F10, in contrast to the M.P, exhibited a statistically significant difference ( $P < 0.05$ ) in the cumulative drug permeation, and F10

demonstrated a drug permeation percentage of 16.87% and a Jss of 0.065  $\mu\text{g}/\text{cm}^2\cdot\text{h}$ , whereas M.P showed a drug permeation percentage of 4.80% and a Jss of 0.015  $\mu\text{g}/\text{cm}^2\cdot\text{h}$ . Conversely, when F6 was compared to M.P, it exhibited no significant result ( $P > 0.05$ ) in the cumulative drug permeation, yielding a drug penetration percentage of 7.95% and a Jss of 0.032  $\mu\text{g}/\text{cm}^2\cdot\text{h}$ . Furthermore, the lag times for F6, F10, and M.P T lag were 4.7 minutes, 3.7 minutes, and 4.5 minutes, respectively, with no significant difference seen ( $P > 0.05$ ) among them (Figure 3).

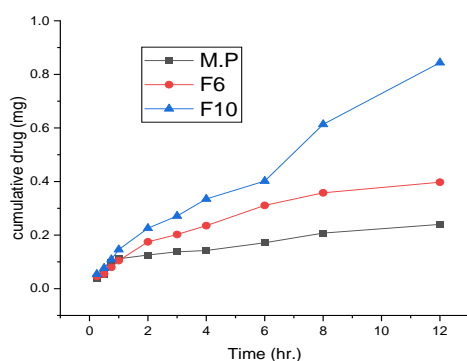


**Figure (3):** Cumulative permeation of optimized inserts F6 and F10 in comparison to M.P

According to the previous results, F10 exhibited an approximate fourfold improvement relative to M.P. and a twofold improvement compared to F6 in terms of the cumulative amount of SAC permeated.

The improvement in corneal drug permeability for both F6 and F10 is likely due to the intrinsic weak bio-adhesion characteristics of EU. RL PO, with this effect being more prominent in F10 than in F6 due to its PVP K90 content, which offers a synergistic enhancement in bio-adhesion (57).

Based on the abovementioned evidence, F10 was selected as the preferable candidate for additional investigation.

### Mechanical characteristics:

The tensile properties (tensile strength and percentage elongation at break) are utilized to evaluate the mechanical qualities of the formulated inserts. These parameters are essential as the produced inserts experience minor stress from the action of blinking and during their handling and insertion in the eye(58).

F10 exhibited a low tensile strength of  $2.227 \pm 0.23$  (N/mm<sup>2</sup>) and a high percent elongation of  $213.88\% \pm 0.211$ , characteristics that are particularly advantageous for enduring modest stress induced by the action of blinking and during handling and placement (59, 60).

### Sterility test and post-UV evaluations:

The ocular environment is sterile; therefore, sterilization is essential for ocular dosage forms(61). Fortunately, TSA and TB demonstrated no evidence of bacterial proliferation or turbidity throughout the incubation period, so validating the efficacy of the UV sterilizing technique. The evaluated F10 inserts can be reliably utilized in animal ocular irritation tests for subsequent examination(28).

Post-UV assessments were conducted, and the findings indicated no significant differences ( $p > 0.05$ ) in tensile strength ( $1.982 \pm 0.043$ ), folding endurance (over 300), percent elongation ( $238.05\% \pm 0.228$ ), drug content ( $4.922 \pm 0.205$ ), drug content percentage ( $98.448 \pm 0.041$ ), and pH ( $6.96 \pm 0.01$ ) relative to the initial evaluation values(27).

### Ocular irritation test:

The insert was positioned in the upper conjunctival sac of the rabbits' eyes. The procedure was performed directly using sterile forceps, without any invasive measures such as surgery, anesthesia, or stitches. A few minutes after insertion, some tearing was observed; however, within fifteen minutes, it continued to diminish gradually until it reached normality. Furthermore, at the conclusion of the test, the conjunctiva, cornea, and iris exhibit no ocular injury or clinical abnormalities. Furthermore, it is generally acknowledged that the rabbit's eye exhibits greater susceptibility to irritating substances compared to the human eye, hence reinforcing the safety of inserts should any clinical research be conducted(62).

The F10 ocular irritation test, earlier described scoring system, received a score of 0 (0 = no alteration) on a 3-point scale, exhibiting no evidence of ocular damage or atypical clinical symptoms in the cornea, iris, or conjunctivae, thereby affirming the insert's safety (Figure 4) (63).

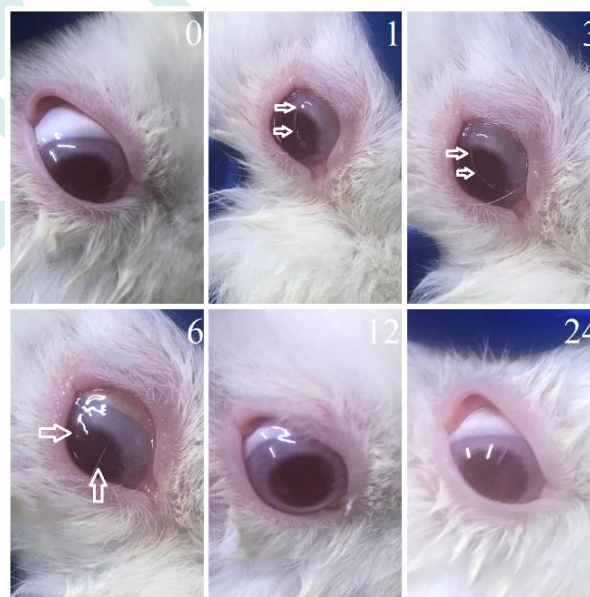


**Figure (4):** In vivo irritation. The numbers denote the post-insertion interval, and arrows point to insert margins.

### Compatibility and Stability studies

DSC is regarded as a sensitive and reliable method for detecting drug polymorphism, melting behavior, and drug-polymer interactions(64). The DSC study of Eu. RL PO reveals a glass transition temperature of around 70 °C. However, based on the purity, it may have a peak about 268.85°C (65, 66). Furthermore, Alg exhibits just two distinct thermal characteristics due to its amorphous nature: dehydration at approximately 100 °C and exothermic decomposition within the range of 240–260 °C, lacking any obvious endothermic peak(67). PVP K90 exhibits a singular broad endothermic curve commencing at roughly 80

°C and concluding around 175.0 °C, signifying the end of the melting process(68, 69). The SAC has a pronounced endothermic peak at 267-269 °C. Ultimately, the comprehensive data previously presented, when paralleled with (F10) DSC data, revealed the elimination of the distinctive SAC peak, signifying the lack of SAC crystallinity and validating the transition to an amorphous state(70) (Figure 5-A)

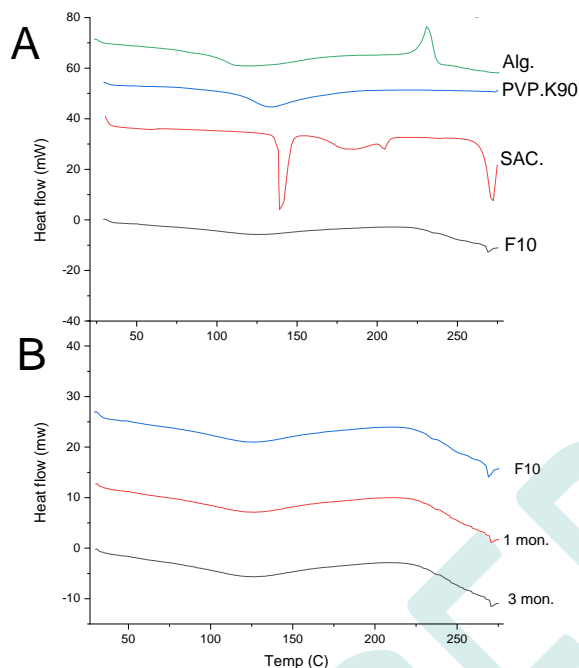


**Figure (6):** DSC data A) formulated F10, SAC, Alg., PVP K90, and Eud RLPO. B) F10 against 1 month and 3 months

In the FTIR analysis, PVP K90 exhibits a distinct C–H stretching peak at 2918  $\text{cm}^{-1}$ , a C=O stretching peak at 1614  $\text{cm}^{-1}$ , and a C–N stretching peak approximately at 1500  $\text{cm}^{-1}$  (71, 72). Alg. exhibits a distinctive broad stretching vibration band of the OH group at 3251  $\text{cm}^{-1}$ , accompanied by an absorption peak at 2933  $\text{cm}^{-1}$ , which is specific to the stretching vibration of C–H bonds(73). A stretching band of the C–O–C glycosidic bond is observed at 1025  $\text{cm}^{-1}$ , together with characteristic absorption peaks at 1616  $\text{cm}^{-1}$  and 1418  $\text{cm}^{-1}$ , which correspond to the asymmetric and symmetric stretching vibrations of  $\text{COO}^-$ , respectively(74, 75). Eud. RLPO has a distinct C–H stretching at 2993  $\text{cm}^{-1}$ , C=O stretching at 1727  $\text{cm}^{-1}$ , N–H stretching vibration of tertiary amine at 3432.1  $\text{cm}^{-1}$ , C=O (ester) stretching at 1731.4  $\text{cm}^{-1}$ , and  $-\text{CH}_3$  bending at 1450.2  $\text{cm}^{-1}$ (76, 77). SAC FTIR typically exhibits asymmetric

and symmetric stretching frequencies of amine hydrogen (N–H) at 3471.2 and 3257.0  $\text{cm}^{-1}$ , respectively. Nevertheless, it was

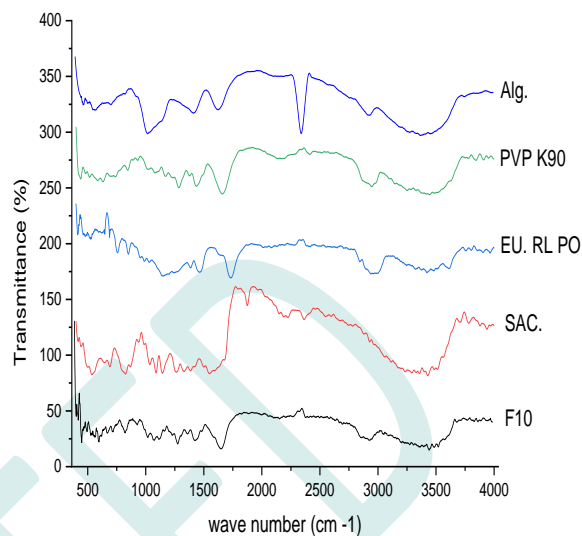


**Figure (5):** FTIR analysis of insert component per and post-formulation

obscured by the extensive and intense water –OH stretching above 3000  $\text{cm}^{-1}$ . SAC exhibits a carbonyl (C=O) stretching at 1678.4  $\text{cm}^{-1}$ , a symmetrical sulfonyl (O=S=O) group at 1642  $\text{cm}^{-1}$ , 1596.18  $\text{cm}^{-1}$ , 1505.61  $\text{cm}^{-1}$ , 1440.51  $\text{cm}^{-1}$ , 1375.01  $\text{cm}^{-1}$ , and 1322.8  $\text{cm}^{-1}$ , and an asymmetrical sulfonyl (O=S=O) group at 1233  $\text{cm}^{-1}$  and 1155  $\text{cm}^{-1}$ (78-80). Ultimately, F10 exhibits heightened intensity and a shift from 1678 to 1660 in the carbonyl region, alongside red shifting and peak enhancement within the O–H stretch region (3000–3700), strongly indicating hydrogen bond formation between the SAC amide carbonyl and the alginate hydroxyl groups(81, 82) (Figure 6).

No chemical interaction or incompatibility was observed according to the FTIR analysis.

Analysis of DSC data over a three-month period indicates that short-term stability is exhibited by no evidence of SAC recrystallization that could influence the drug release profile (Figure 5-B). The hydrogen bonding between Alg and SAC, as indicated by FTIR analysis, may improve the stability of SAC's amorphous form within the polymeric matrix, therefore inhibiting phase separation and favorably impacting the short-term stability assessment at 25°C(83). The overall assessment criteria during short-term storage indicate no significant differences in tensile strength ( $P > 0.05$ ), percent elongation ( $P > 0.05$ ), drug content ( $P > 0.05$ ), content percentage ( $P > 0.05$ ), and pH ( $P > 0.05$ ) (Figure 4).

**Table (4):** SAC ocular insert (F10) short-term stability evaluation parameters and results.

parameters	Tensile strength (N/mm <sup>2</sup> )	percent elongation (%)	drug content(mg)	Content percentage (%)	PH	Folding endurance
Day zero storage	2.227±0.231	213.88%±0.211	4.827±0.242	96.552±0.048	6.97±0.02	over 300
30days storage	2.229±0.194	198.68%±0.287	4.858±0.215	97.176±0.043	6.96±0.02	over 300
90days storage	1.922±0.091	178.18%±0.484	4.801±0.160	96.408±0.030	6.96±0.02	over 300



## Conclusion

The SAC biodegradable ocular insert was effectively produced with a matrix layer comprising 1.5% (w/v) alginate and 7% (w/v) PVP K90, coated with a rate-controlling layer of 15% (w/v) Eud RLPO and 5% (w/v) PVP K90. This formulation achieved a sustained SAC release duration of 12 hours, complying with zero-order kinetics, with complete biodegradation of the insert and a fourfold increase in corneal permeation. These qualities significantly decrease the frequency of drug delivery from 12 times, as observed with typical eye drop solutions, to merely twice daily and ensure a consistent drug release devoid of daily fluctuations, hence reducing any adverse effects and also eliminating the necessity for insert recovery after insertion. These data strongly suggest that SAC ocular insert may enhance patient compliance relative to conventional ocular preparations. The improvement in corneal permeability may facilitate the future application of SAC ocular inserts in the treatment of bacterial keratitis for future studies.

## Ethics approval and consent to participate

The Institutional Ethical Committee- Department of Pharmacy, al Mustansiriyyah University reviewed and approved the protocol.

## Availability of data and materials

Supplementary data can be shared upon reasonable request

## Author's contribution

Haider H. Kikawoos contributed to data gathering, analysis, and practical and written parts of the study. Athmar DH. H. Al-Shohani: final approval and agreement for all aspects of the research, supervision, revision, and rearrangement.

## Funding

This research received no specific grant from any funding agency.

## Conflicts of interest

The authors have no conflict of interest to declare.

## Acknowledgements

The authors would like to express their gratitude to Mustansiriyyah University/College of Pharmacy and all participants for contributing to the study

## Open Access

This article is licensed under a Creative Commons Attribution 4.0 International License, which permits use, sharing, adaptation, distribution and reproduction in any medium or format, as long as you give appropriate credit to the original author(s) and the source, provide a link to the Creative Commons licence, and indicate if changes were made. The images or other third party material in this article are included in the article's Creative Commons licence, unless indicated otherwise in a credit line to the material. If material is not included in the article's Creative Commons licence and your intended use is not permitted by statutory regulation or exceeds the permitted use, you will need to obtain permission directly from the copyright holder. To view a copy of this license, visit <https://creativecommons.org/licenses/by-nc/4.0/>

## References

1] Al-Eryani SA, Alshamahi EYA, Al-Shamahy HA, Alfalahi GHA, Al-Rafiq AA. Bacterial conjunctivitis of adults: causes and ophthalmic antibiotic

- resistance patterns for the common bacterial isolates. *Uni J Pharma Res.* 2021;6(1):25-8.doi:10.22270/ujpr.v6i1.535
- 2] Sensoy D, Cevher E, Sarici A, Yilmaz M, Özdamar A, Bergişadi N. Bioadhesive sulfacetamide sodium microspheres: Evaluation of their effectiveness in the treatment of bacterial keratitis caused by *Staphylococcus aureus* and *Pseudomonas aeruginosa* in a rabbit model. *European Journal of Pharmaceutics and Biopharmaceutics.* 2009;72(3):487-95.<https://doi.org/10.1016/j.ejpb.2009.02.006>
- 3] Wang Y, Wang C. Novel eye drop delivery systems: advance on formulation design strategies targeting anterior and posterior segments of the eye. *Pharmaceutics.* 2022;14(6):1150.doi: 10.3390/pharmaceutics14061150.
- 4] Grassiri B, Zambito Y, Bernkop-Schnürch A. Strategies to prolong the residence time of drug delivery systems on ocular surface. *Advances in Colloid and Interface Science.* 2021;288:102342.<https://doi.org/10.1016/j.cis.2020.102342>
- 5] Noor Hameed A, Nidhal Khazaal M. Insights into medicated films as attractive dosage forms. *Al Mustansiriyyah Journal of Pharmaceutical Sciences.* 2023;23(1):1-13.10.32947/ajps.v23i1.981
- 6] Mofidfar M, Abdi B, Ahadian S, Mostafavi E, Desai TA, Abbasi F, et al. Drug delivery to the anterior segment of the eye: A review of current and future treatment strategies. *Inter j pharma.* 2021;607:120924.doi: 10.1016/j.ijpharm.2021.120924.
- 7] Karthikeyan D, Bhowmick M, Pandey VP, Nandhakumar J, Sengottuvelu S, Sonkar S, et al. The concept of ocular inserts as drug delivery systems: An overview. *Asian Journal of Pharmaceutics (AJP).* 2014;2(4).10.22377/ajp.v2i4.204
- 8] Kumari B. Ocular drug delivery system: Approaches to improve ocular bioavailability. *GSC Biological and Pharmaceutical Sciences.* 2019;6(3):01-010.10.30574/gscbps.2019.6.3.0030
- 9] Kurade DS, Joshi D, Anita B. A review on ocular drug delivery with new trends. *International Journal of Advanced Research.* 2015;3(11):629-42
- 10] Alzahrani A, Youssef AAA, Nyavanandi D, Tripathi S, Bandari S, Majumdar S, et al. Design and optimization of ciprofloxacin hydrochloride biodegradable 3D printed ocular inserts: Full factorial design and in-vitro and ex-vivo evaluations: Part II. *International Journal of Pharmaceutics.* 2023;631:122533.<https://doi.org/10.1016/j.ijpharm.2022.122533>
- 11] Borbolla-Jiménez FV, Peña-Corona SI, Farah SJ, Jiménez-Valdés MT, Pineda-Pérez E, Romero-Montero A, et al. Films for Wound Healing Fabricated Using a Solvent Casting Technique. *Pharmaceutics.* 2023;15(7):1914.doi: 10.3390/pharmaceutics15071914
- 12] Aburahma MH, Mahmoud AA. Biodegradable ocular inserts for sustained delivery of brimonidine tartrate: preparation and in vitro/in vivo evaluation. *Aaps Pharm.* 2011;12:1335-47.doi: 10.1208/s12249-011-9701-3
- 13] Teaima M, Yasser M, Elfar N, Shoueir K, El-Nabarawi M, Helal D. Construction of sublingual trilaminated Eszopiclone fast dissolving film for the treatment of Insomnia: Formulation, characterization and In vivo clinical comparative pharmacokinetic study in healthy human subjects. *Plos one.* 2022;17(6):e0266019.doi: 10.1371/journal.pone.0266019.
- 14] Ramadan AEh, Elsayed MMA, Elsayed A, Fouad MA, Mohamed MS, Lee S, et al. Development and optimization of vildagliptin solid lipid nanoparticles loaded ocuserts for controlled ocular delivery: A promising approach towards treating diabetic retinopathy. *Inter J Pharma X.* 2024;7:100232.doi: 10.1016/j.ijpx.2024.100232
- 15] Mahrous GM, Shazly G, Zidan DE, Abdel Zaher AA, El-Mahdy M. Formulation and evaluation of buccoadhesive films of lidocaine hydrochloride. *J adv Bio I Pharma Sci.* 2020;3(2):53-9.doi: 10.21608/JABPS.2020.21927.1066
- 16] Al-Mogherah AI, Ibrahim MA, Hassan MA. Optimization and evaluation of venlafaxine hydrochloride fast dissolving oral films. *Sau pharma j.* 2020;28(11):1374-82.doi: 10.1016/j.jsps.2020.09.001
- 17] Gajbhiye K, Hakam N, Rathod G, Tawar M. Formulation and evaluation of transdermal patches of benidipine hydrochloride. *Asian J Ph I Tech.* 2021;11(3):207-12.doi: 10.52711/2231-5713.2021.00034
- 18] Mohamad SA, Salem H, Yassin HA, Mansour HF. Bucco-adhesive film as a pediatric proper dosage form for systemic delivery of propranolol hydrochloride: In-vitro and in-vivo evaluation. *Drug des dev I therapy.* 2020:4277-89.doi: 10.2147/DDDT.S267317
- 19] Zafar A, Imam SS, Yasir M, Alruwaili NK, Alsaïdan OA, Warsi MH, et al. Preparation of NLCs-Based Topical Erythromycin Gel: In Vitro Characterization and Antibacterial Assessment. *Gels.* 2022;8(2).doi: 10.3390/gels8020116
- 20] Nagpal MA, Sharma K, Anand N, Singh D, Dhawan R, Usman MRM, et al. Preparation and evaluation of sulfacetamide sodium ocusert for controlled drug delivery. *J Drug Del I Thera.* 2020;10(2):164-70.doi: 10.22270/jddt.v10i2.3928
- 21] Dayoub RA, Laham A. Preparation and In-vitro Evaluation of Timolol Maleate Loaded Ocular inserts by using various polymers. *Res J Pharma I Tech.* 2023;16(3):1259-66.doi: 10.52711/0974-360X.2023.00208
- 22] Safa Mohammed N, Athmar Dhahir Habeeb A-S, Alaa A. Effect of using high molecular weight crosslinker on the physical properties of super porous hydrogel composite. *Al Mustansiriyyah Journal of Pharmaceutical Sciences.* 2023;23(4):355-66.10.32947/ajps.v23i4.1091

- 23] Mady OY, Abulmeaty MM, Donia AA, Al-Khureif AA, Al-Shoubki AA, Abudawood M, et al. Formulation and bioavailability of novel mucoadhesive buccal films for candesartan cilexetil in rats. *Membranes*. 2021;11(9):659. doi: 10.3390/membranes11090659
- 24] Patil SS, Bade A, Tagalpallewar A. Design, optimization and pharmacodynamic comparison of dorzolamide hydrochloride soluble ocular drug insert prepared by using 32 factorial design. *J Drug Del Sci I Tech*. 2018;46:138-47. doi: 10.1016/j.jddst.2018.05.010
- 25] Di Prima G, Licciardi M, Bongiovanni F, Pitarresi G, Giammona G. Inulin-Based Polymeric Micelles Functionalized with Ocular Permeation Enhancers: Improvement of Dexamethasone Permeation/Penetration through Bovine Corneas. *Pharma*. 2021;13(9).doi: 10.3390/pharmaceutics13091431
- 26] Racaniello GF, Pistone M, Meazzini C, Lopodota A, Arduino I, Rizzi R, et al. 3D printed mucoadhesive orodispersible films manufactured by direct powder extrusion for personalized clobetasol propionate based paediatric therapies. *Inter J Pharma*. 2023;643:123214. doi: 10.1016/j.ijpharm.2023.123214
- 27] Taghe S, Mirzaeei S, Bagheri M. Preparation of polycaprolactone and polymethacrylate nanofibers for controlled ocular delivery of ketorolac tromethamine: Pharmacokinetic study in Rabbit's Eye. *Eu J Pharma Sci*. 2024;192:106631. doi: 10.1016/j.ejps.2023.106631
- 28] Guadarrama-Escobar OR, Valdés-Alvarez CA, Constantino-Gonzalez KS, Serrano-Castañeda P, Peña-Juárez MC, Morales-Florido MI, et al. Design and Characterization of Ocular Inserts Loaded with Dexamethasone for the Treatment of Inflammatory Ophthalmic Disease. *Pharmaceutics*. 2024;16(2):294. doi: 10.3390/pharmaceutics16020294
- 29] Khairnar S, Sanchez-Lopez E, Souto EB, Singh KK. Moxifloxacin loaded microspheres-composed gel for controlled release and enhanced penetration in ocular tissues: In vitro, ex vivo and in vivo proof of concept. *J Drug Del Sci I Tech*. 2023;90:105111. doi: 10.1016/j.jddst.2023.105111
- 30] Abd El-Bary A, Kamal Ibrahim H, Haza'a BS, Al Sharabi I. Formulation of sustained release bioadhesive minitablets containing solid dispersion of levofloxacin for once daily ocular use. *Pharma Dev I Tech*. 2019;24(7):824-38. doi: 10.1080/10837450.2019.1602631
- 31] Taghe S, Mirzaeei S, Ahmadi A. Preparation and Evaluation of Nanofibrous and Film-Structured Ciprofloxacin Hydrochloride Inserts for Sustained Ocular Delivery: Pharmacokinetic Study in Rabbit's Eye. *Life*. 2023;13(4):913. doi: 10.3390/life13040913
- 32] Sun X, Yu Z, Cai Z, Yu L, Lv Y. Voriconazole composited polyvinyl alcohol/hydroxypropyl-β-cyclodextrin nanofibers for ophthalmic delivery. *PLoS one*. 2016;11(12):e0167961. doi: 10.1371/journal.pone.0167961
- 33] Tekko IA, Chen G, Domínguez-Robles J, Thakur RRS, Hamdan IM, Vora L, et al. Development and characterisation of novel poly (vinyl alcohol)/poly (vinyl pyrrolidone)-based hydrogel-forming microneedle arrays for enhanced and sustained transdermal delivery of methotrexate. *International journal of pharmaceutics*. 2020;586:119580
- 34] Nair AB, Singh B, Shah J, Jacob S, Aldhubiab B, Sreeharsha N, et al. Formulation and Evaluation of Self-Nanoemulsifying Drug Delivery System Derived Tablet Containing Sertaline. *Pharmaceutics*. 2022;14(2).10.3390/pharmaceutics14020336
- 35] Araújo AAS, Bezerra MdS, Storpirtis S, Matos JdR. Determination of the melting temperature, heat of fusion, and purity analysis of different samples of zidovudine (AZT) using DSC. *Brazilian Journal of Pharmaceutical Sciences*. 2010;46:37-43
- 36] F Z, R R, K S. A REVIEW ON STABILITY TESTING GUIDELINES OF PHARMACEUTICAL PRODUCTS. *Asian Journal of Pharmaceutical and Clinical Research*. 2020;13(10):3-9.10.22159/ajpcr.2020.v13i10.38848
- 37] Karnik I, Youssef AAA, Joshi P, Munnangi SR, Narala S, Varner C, et al. Formulation development and characterization of dual drug loaded hot-melt extruded inserts for better ocular therapeutic outcomes: Sulfacetamide/prednisolone. *J Drug Del Sci I Tech*. 2023;84:104558. doi: 10.1016/j.jddst.2023.104558
- 38] Bao Z, Yu A, Shi H, Hu Y, Jin B, Lin D, et al. Glycol chitosan/oxidized hyaluronic acid hydrogel film for topical ocular delivery of dexamethasone and levofloxacin. *Int J Biol Macromol*. 2021;167:659-66.10.1016/j.ijbiomac.2020.11.214
- 39] Lisa Land D, Benjamin WJ. Sizes and shapes of conjunctival inserts. *International Contact Lens Clinic*. 1994;21(11):212-7. [https://doi.org/10.1016/0892-8967\(94\)90053-1](https://doi.org/10.1016/0892-8967(94)90053-1)
- 40] Saettone MF, Salminen L. Ocular inserts for topical delivery. *Advanced Drug Delivery Reviews*. 1995;16(1):95-106. [https://doi.org/10.1016/0169-409X\(95\)00014-X](https://doi.org/10.1016/0169-409X(95)00014-X)
- 41] Gevariya H, Dharamsi A, Girhepunje K, Pal R. Once a day ocular inserts for sustained delivery of levofloxacin: Design, formulation and evaluation. *Asian J f Pharma*. 2014;3(4).doi: 10.22377/ajp.v3i4.286
- 42] Gevariya H, Dharamsi A, Girhepunje K, Pal R. Once a day ocular inserts for sustained delivery of levofloxacin: Design, formulation and evaluation. *Asian Journal of Pharmaceutics*. 2009;3.10.4103/0973-8398.59954
- 43] Boateng JS, Popescu AM. Composite bi-layered erodible films for potential ocular drug delivery. *Colloids and Surfaces B: Biointerfaces*. 2016;145:353-61. <https://doi.org/10.1016/j.colsurfb.2016.05.014>
- 44] Dawaba A, Dawaba H, El-Enin A, Khalifa M. Fabrication of bioadhesive ocusert with different polymers: Once a day dose. *International Journal of Applied Pharmaceutics*. 2018;10:309.10.22159/ijap.2018v10i6.28495
- 45] Gupta NV, Reddy G. A Comparative study of quality control tests for eye preparations as per IP, BP and USP. *Int J Drug Dev & Res*. 2015;7:0975-9344
- 46] Guadarrama-Escobar OR, Valdés-Alvarez CA, Constantino-Gonzalez KS, Serrano-Castañeda P, Peña-Juárez MC, Morales-Florido MI, et al. Design and Characterization of Ocular Inserts Loaded with Dexamethasone for the Treatment of Inflammatory Ophthalmic Disease. *Pharmaceutics*. 2024;16(2):294
- 47] Mariz M, Murta J, Gil MH, Ferreira P. An ocular insert with zero-order extended delivery: Release kinetics and mathematical models. *European Journal of Pharmaceutics and Biopharmaceutics*. 2022;181:79-87. <https://doi.org/10.1016/j.ejpb.2022.10.023>
- 48] dos Santos J, da Silva GS, Velho MC, Beck RC. Eudragit®: A Versatile Family of Polymers for Hot Melt Extrusion and 3D Printing Processes in Pharmaceutics. *Pharma*. 2021;13(9).doi: 10.3390/pharmaceutics13091424
- 49] Maulvi FA, Patel PJ, Soni PD, Desai AR, Desai DT, Shukla MR, et al. Novel Poly(vinylpyrrolidone)-Coated Silicone Contact Lenses to Improve Tear Volume During Lens Wear: In Vitro and In Vivo Studies. *ACS Omega*. 2020;5(29):18148-54. doi: 10.1021/acsomega.0c01764
- 50] Boateng JS, Popescu AM. Composite bi-layered erodible films for potential ocular drug delivery. *Collo Surf B: Biointerfaces*. 2016;145:353-61. doi: 10.1016/j.colsurfb.2016.05.014
- 51] Maderuelo C, Zarzuelo A, Lanao JM. Critical factors in the release of drugs from sustained release hydrophilic matrices. *J Con Rel*. 2011;154(1):2-19. doi: 10.1016/j.jconrel.2011.04.002
- 52] Nikam A, Sahoo PR, Musale S, Pagar RR, Paiva-Santos AC, Giram PS. A Systematic Overview of Eudragit® Based Copolymer for Smart Healthcare. *Pharmaceutics*. 2023;15(2).doi: 10.3390/pharmaceutics15020587
- 53] Jumelle C, Gholizadeh S, Annabi N, Dana R. Advances and limitations of drug delivery systems formulated as eye drops. *J Con Rel*. 2020;32(1):1-22. doi: 10.1016/j.jconrel.2020.01.057
- 54] Brazel CS, Peppas NA. Mechanisms of solute and drug transport in relaxing, swellable, hydrophilic glassy polymers. *Polymer*. 1999;40(12):3383-98. [https://doi.org/10.1016/S0032-3861\(98\)00546-1](https://doi.org/10.1016/S0032-3861(98)00546-1)
- 55] Bin-Jumah M, Gilani SJ, Jahangir MA, Zafar A, Alshehri S, Yasir M, et al. Clarithromycin-Loaded Ocular Chitosan Nanoparticle: Formulation, Optimization, Characterization, Ocular Irritation, and Antimicrobial Activity. *Int J Nanomedicine*. 2020;15:7861-75.10.2147/ijn.S269004
- 56] Swain R, Moharana A, Habibullah S, Nandi S, Bose A, Mohapatra S, et al. Ocular delivery of felodipine for the management of intraocular pressure and inflammation: Effect of film plasticizer and in vitro in vivo evaluation. *International Journal of Pharmaceutics*. 2023;642:123153. <https://doi.org/10.1016/j.ijpharm.2023.123153>
- 57] Bin-Jumah M, Gilani SJ, Jahangir MA, Zafar A, Alshehri S, Yasir M, et al. Clarithromycin-Loaded Ocular Chitosan Nanoparticle: Formulation, Optimization, Characterization, Ocular Irritation, and Antimicrobial Activity. *Inter J Nano*. 2020;15(null):7861-75. doi: 10.2147/IJN.S269004
- 58] Cegielska O, Sierakowski M, Sajkiewicz P, Lorenz K, Kogermann K. Mucoadhesive brinzolamide-loaded nanofibers for alternative glaucoma treatment. *European Journal of Pharmaceutics and Biopharmaceutics*. 2022;180:48-62. <https://doi.org/10.1016/j.ejpb.2022.09.008>
- 59] Cegielska O, Sierakowski M, Sajkiewicz P, Lorenz K, Kogermann K. Mucoadhesive brinzolamide-loaded nanofibers for alternative glaucoma treatment. *Eur J Pharma I Biopharma*. 2022;180:48-62. doi: 10.1016/j.ejpb.2022.09.008
- 60] Noori MM, Al-Shohani ADHH, Yousif NZ. Fabrication and characterization of new combination ocular insert for the combined delivery of tinidazole and levofloxacin. *Materials Today: Proceedings*. 2023;80:2652-9. doi: 10.1016/j.matpr.2021.07.008
- 61] Aminu N, Mohammed KG, Ilyasu S, Yahaya Z, Shuaibu F, Nuhu T, et al. Pharmaceutical sterile formulations. 2024. p. 577-611.
- 62] Asfour MH, Abd El-Alim SH, Awad GEA, Kassem AA. Chitosan/β-glycerophosphate in situ forming thermo-sensitive hydrogel for improved ocular delivery of moxifloxacin hydrochloride. *Eur J Pharm Sci*. 2021;167:106041.10.1016/j.ejps.2021.106041
- 63] Charneau-Genevois C, Sarang S, Perea M, Mayer N, Eadsforth C, Austin T, et al. A simplified index to quantify the irritation/corrosion potential of chemicals – Part II: Eye. *Regulatory Toxicology and Pharmacology*. 2021;123:104935. <https://doi.org/10.1016/j.yrtph.2021.104935>
- 64] Meiland P, Larsen BS, Knopp MM, Tho I, Rades T. A new method to determine drug-polymer solubility through enthalpy of melting and mixing. *International Journal of Pharmaceutics*. 2022;629:122391. <https://doi.org/10.1016/j.ijpharm.2022.122391>
- 65] Thakur N, Kaur B, Goswami M, Sharma C. Compatibility studies of the Thiocolchicoside with Eudragit RLPO, Eudragit E100 and Eudragit L100 using thermal and non-thermal methods. *Drug Combination Therapy*. 2022;4:1.10.53388/DCT2021100301
- 66] Balagani PK, Chandiran I, Jayaveera KN. Formulation development and evaluation of Glibenclamide loaded Eudragit RLPO microparticles.

- 67] Palo M, Rönköharju S, Tiirik K, Viidik L, Sandler N, Kogermann K. Bi-Layered Polymer Carriers with Surface Modification by Electrospinning for Potential Wound Care Applications. *Pharmaceutics*. 2019;11(12):678
- 68] Laosirisathian N, Saenjum C, Sirithunyalug J, Eitssayeam S, Chaiyana W, Sirithunyalug B. PVA/PVP K90 Nanofibers Containing Punica granatum Peel Extract for Cosmeceutical Purposes. *Fibers and Polymers*. 2021;22(1):36-48.10.1007/s12221-021-0165-0
- 69] Gilhotra RM, Gilhotra N, Mishra DN. Piroxicam Bioadhesive Ocular Inserts: Physicochemical Characterization and Evaluation in Prostaglandin-Induced Inflammation. *Current Eye Research*. 2009;34(12):1065-73.10.3109/02713680903340738
- 70] Mohammed SH, Ali WK. Preparation and characterization of taste masked valsartan by ion-exchange resin approach. *Al Mustansiriyah Journal of Pharmaceutical Sciences*. 2018;18(1):11-25.10.32947/ajps.v18i1.453
- 71] Adam AA, Ali MKM, Dennis JO, Soleimani H, Shukur MFBA, Ibaouf KH, et al. Innovative Methylcellulose-Polyvinyl Pyrrolidone-Based Solid Polymer Electrolytes Impregnated with Potassium Salt: Ion Conduction and Thermal Properties. *Polymers*. 2022;14(15):3055
- 72] Liu H, Jiang W, Yang Z, Xiren C, Yu D, Shao J. Hybrid Films Prepared from a Combination of Electrospinning and Casting for Offering a Dual-Phase Drug Release. *Polymers*. 2022;14:2132.10.3390/polym14112132
- 73] Moura-Alves M, Souza VGL, Silva JA, Esteves A, Pastrana LM, Saraiva C, et al. Characterization of Sodium Alginate-Based Films Blended with Olive Leaf and Laurel Leaf Extracts Obtained by Ultrasound-Assisted Technology. *Foods*. 2023;12(22):4076
- 74] Derkach S, Voron'ko N, Sokolan N, Kolotova D, Kuchina Y. Interactions between gelatin and sodium alginate: UV and FTIR studies. *Journal of Dispersion Science and Technology*. 2019;41:1-9.10.1080/01932691.2019.1611437
- 75] Kilicarslan M, Ilhan M, Inal O, Orhan K. Preparation and evaluation of clindamycin phosphate loaded chitosan/alginate polyelectrolyte complex film as mucoadhesive drug delivery system for periodontal therapy. *European Journal of Pharmaceutical Sciences*. 2018;123:441-51.<https://doi.org/10.1016/j.ejps.2018.08.007>
- 76] Mehta R, Chawla A, Sharma P, Pawar P. Formulation and in vitro evaluation of Eudragit S-100 coated naproxen matrix tablets for colon-targeted drug delivery system. *J Adv Pharm Technol Res*. 2013;4(1):31-41.10.4103/2231-4040.107498
- 77] Kim W, Ngo HV, Nguyen HD, Park J-M, Lee KW, Park C, et al. Nanonization and Deformable Behavior of Fattigated Peptide Drug in Mucoadhesive Buccal Films. *Pharmaceutics*. 2024;16(4):468
- 78] Abilova GK, Kaldybekov DB, Irmukhametova GS, Kazymbayeva DS, Iskabayeva ZA, Kudaibergenov SE, et al. Chitosan/Poly(2-ethyl-2-oxazoline) Films with Ciprofloxacin for Application in Vaginal Drug Delivery. *Materials (Basel)*. 2020;13(7).10.3390/ma13071709
- 79] Nagula RG, Khan R, Nangia A. Modulating the solubility of sulfacetamide by means of cocrystals. *CrystEngComm*. 2014;16:5859.10.1039/c4ce00103f
- 80] Mandal B, Alexander KS, Riga AT. Sulfacetamide loaded Eudragit® RL100 nanosuspension with potential for ocular delivery. *J Pharm Pharm Sci*. 2010;13(4):510-23
- 81] Saboo S, Kestur US, Flaherty DP, Taylor LS. Congruent Release of Drug and Polymer from Amorphous Solid Dispersions: Insights into the Role of Drug-Polymer Hydrogen Bonding, Surface Crystallization, and Glass Transition. *Mol Pharma*. 2020;17(4):1261-75.doi: 10.1021/acs.molpharmaceut.9b01272
- 82] Karas LJ, Wu C-H, Das R, Wu JI-C. Hydrogen bond design principles. *WIREs Comp Mol Sci*. 2020;10(6):e1477.doi: 10.1002/wcms.1477
- 83] Asfour MH, Abd El-Alim SH, Awad GEA, Kassem AA. Chitosan/β-glycerophosphate in situ forming thermo-sensitive hydrogel for improved ocular delivery of moxifloxacin hydrochloride. *Euro J Pharma Sci*. 2021;167:106041.doi: 10.1016/j.ejps.2021.106041